

Synthesis of Polypyrrole-Modified TiO₂ Composite Adsorbent and Its Adsorption Performance on Acid Red G

Jingjing Li,¹ Jiangtao Feng,^{1,2} Wei Yan^{1,3}

¹Department of Environmental Science and Engineering, Xi'an Jiaotong University, Xi'an 710049, People's Republic of China

²Suzhou Academy of Xi'an Jiaotong University, Suzhou 215021, People's Republic of China

³State Key Laboratory of Multiphase Flow in Power Engineering, Xi'an Jiaotong University, Xi'an 710049, People's Republic of China

Correspondence to: W. Yan (E-mail: yanwei@xjtu.edu.cn)

ABSTRACT: The adsorption–desorption characteristics of Acid Red G (ARG) on the polypyrrole-modified TiO₂ (PPy/TiO₂) composite as a novel adsorbent was investigated. PPy/TiO₂ was synthesized via the *in-situ* polymerization of pyrrole monomer in the prepared TiO₂ sol solution. Results from X-ray diffraction and Fourier transform infrared spectra indicated the formation of the PPy/TiO₂ composite. The adsorption experiments showed that the modification of PPy substantially improved the adsorption and regeneration abilities of PPy/TiO₂. The adsorption equilibrium was achieved in a short time of 20 min, and the adsorption kinetics followed the pseudo-second-order model. The Langmuir adsorption isotherm was found for PPy/TiO₂, with the maximum adsorption capacity of 179.21 mg/g. The regeneration experiments showed that PPy/TiO₂ could be successfully regenerated by simple alkali-acid treatment. The adsorption efficiency of the regenerated PPy/TiO₂ adsorbent for ARG was still greater than 90% after regeneration for 10 times. Additionally, the adsorption efficiency of PPy/TiO₂ for the ARG effluent was still higher than 78% after adsorption–desorption for four times. It is expected that the PPy/TiO₂ composite can be considered as a stable adsorbent for the removal of dye. © 2012 Wiley Periodicals, Inc. *J. Appl. Polym. Sci.* 128: 3231–3239, 2013

KEYWORDS: adsorption; conducting polymers; dyes/pigments

Received 29 May 2012; accepted 26 August 2012; published online 20 September 2012

DOI: 10.1002/app.38525

INTRODUCTION

The printing and dyeing industries yield a large amount of dye wastewater with high color intensity and complex components, which can cause serious water pollution if directly discharged into the environment without appropriate treatment. Dense color can absorb and reflect the sunlight entering water, and consequently interfere with the biological process in water bodies, followed by a water deteriorating matter.^{1–3} Therefore, it is important to remove dyes from dye wastewater.

Recently, various treatment processes have been widely employed to remove dyes from wastewater.⁴ The chemical process may lead to a satisfactory result, but some dye wastewater features low concentration and large amount, which renders the chemical process low efficiency and high cost. Therefore, it is essential for dye wastewater to be concentrated before other methods proceed. Adsorption has been proved to be a reliable treatment approach owing to its low capital investment, abundant raw material source, simplicity of design and operation, and insensitivity to toxic substances.⁵ However, the choice of

appropriate adsorbent for real applications is quite a challenging issue. Many potential adsorbents have been tested for dye wastewater treatment, including polymer,¹ activated carbon,^{6,7} clay and clay minerals,⁸ chitosan,⁹ metal oxides,¹⁰ and biomass,^{11,12} some of them exhibit excellent adsorption properties. Nevertheless, the regeneration of adsorbents without losing adsorption ability is still a great challenge. Although several regeneration methods have been used to regenerate activated carbon, some of them are still deficient, such as carbon loss, low regeneration efficiency, costly operation and immature technology.^{13–15}

Semiconducting titanium dioxide (TiO₂) material has been used in various applications, including solar cells, luminescent materials, photocatalysts, biomaterials, memory devices and adsorbent materials, due to its low cost, simple preparation, good stability, nontoxic nature, and photodegradation ability.¹⁶ Up to now, most of the previous studies have mainly focused on the photocatalytic properties of TiO₂, while the investigation on the adsorption property of TiO₂ is comparatively rare. Actually, TiO₂ can serve as an ideal adsorbent, because the insolubility

and the point of zero charge (pH_{pzc}) at neutral pH value make it possible to study its adsorption capacity over a broad range of pH.¹⁷ Moreover, the hydroxyl and carboxyl groups which present on the surface of TiO_2 can interact with the pollutant molecules, thereby realizing the adsorption of the pollutants.^{18,19} Recently, some publications have focused on the adsorption of organic dyes with TiO_2 , such as Acid Orange 7, Methyl Orange, Reactive Red 195, Reactive Red 198, Direct Green 99, Reactive Black and so on;^{16,19–22} however, not all of them can be effectively adsorbed on the surface of TiO_2 . Moreover, the studies on the regeneration of TiO_2 are extremely rare, which might be due to the sharp decrease of the adsorption capacity of the regenerated TiO_2 . For instance, Asuha et al.¹⁹ reported that the adsorption capacities of the regenerated TiO_2 for Cr(VI) and Methyl Orange were only ca. 50% and 20% of the original values, respectively.

Therefore, the improvement in the adsorption and regeneration capacities through modification with other substances is highly desired. Since the OH groups in TiO_2 do not fully contribute to the ion exchange process, the modification of other substances might combine with partial OH groups without decreasing its adsorption capacity.²³ Polypyrrole (PPy) has been used as sensitizer for TiO_2 in many studies because of its high thermal stability and non-toxicity.²⁴ In fact, it was recognized that PPy also has the adsorption ability through ion exchange or electrostatic interaction, largely owing to the existence of positively charged nitrogen atoms in PPy matrix.^{25–29} Moreover, PPy can undergo protonation or deprotonation reactions when it is immersed in alkali or acid solution, resulting in the change of its surface charges, followed by doping or dedoping of counter ions.^{30,31} The capability of reversible transformation of PPy makes it possible that the ions could be adsorbed on or desorbed from PPy, i.e., it will have an excellent adsorption–desorption property. Therefore, PPy can be considered as a potential modification material of TiO_2 to improve its adsorption and regeneration abilities.

Herein, we synthesized PPy-modified TiO_2 (PPy/ TiO_2) composite adsorbent through the chemical oxidation of pyrrole in the prepared TiO_2 sol solution, and investigated its adsorption and regeneration properties for azo dye, Acid Red G (ARG). Our study found out that the PPy/ TiO_2 composite adsorbent exhibited excellent adsorption and regeneration properties, even after several adsorption–desorption cycles. Furthermore, compared with some other adsorbents, the novel PPy/ TiO_2 composite adsorbent exhibited a fast kinetics and could reach the adsorption equilibrium in a very short time.

EXPERIMENTAL

Materials

Pyrrole (98%, Qingquan Pharmaceutical & Chemical, Zhejiang, China) was distilled twice under reduced pressure, and then refrigerated and stored in the dark under nitrogen. Acid Red G (ARG) was commercial grade and purified before used. $\text{FeCl}_3 \cdot 6\text{H}_2\text{O}$, HNO_3 (65–68%), NaOH, NaCl, n-propanol (99.9%) and tetrabutyl titanate ($\text{Ti}(\text{OC}_4\text{H}_9)_4$, 98%) were of analytical reagent grades and used without further purification. The real effluent used in our study was derived from the printing

and dyeing factory in Xi'an ($\text{pH} = 3.4$), and its colority was relatively low. The deionized water used for all the experiments was obtained by an EPED-40TF Superpure Water System (EPED, China).

Synthesis of Adsorbents

PPy/ TiO_2 was prepared by the chemical oxidative polymerization of pyrrole monomer in the prepared TiO_2 sol solution. The TiO_2 sol solution was prepared by sol–gel hydrolysis, and the process was described as follows. First, a mixture of 20 mL $\text{Ti}(\text{OC}_4\text{H}_9)_4$ and 8 mL n-propanol was added dropwise into 400 mL HNO_3 solution ($\text{pH} = 0.8$, 65°C) with magnetic stirring. Then, a uniform and transparent sol solution was formed, followed by cooling down to room temperature with continuously stirring. Afterwards, the sol solution was transferred to a 500-mL three-neck round bottom flask and cooled to $0\text{--}5^\circ\text{C}$ with mechanical stirring. Then pyrrole (0.25 mL) monomer was added to the sol and stirred for 30 min, followed by adding 10 mL FeCl_3 (1.0 mol/L) solution dropwise under mechanical stirring for 1 h. Then the mixed solution was reacted for an additional 24 h at $0\text{--}5^\circ\text{C}$ statically. Finally, the PPy/ TiO_2 composite was centrifuged at 4500 rpm for 10 min and washed with deionized water, and then dried at ambient temperature for 48 h.

For comparison, the pure TiO_2 was prepared by adding 10 mL NaOH solution (1.0 mol/L) into the as-prepared TiO_2 sol, and then washed with plenty of deionized water and finally dried at ambient temperature for 48 h.

Characterization

XRD diffraction of the samples was obtained from an X'Pert PRO MRD Diffractometer using $\text{Cu-K}\alpha$ radiation. FTIR spectra of samples were measured by the KBr pellet method on a BRUKER TENSOR 37 FT-IR spectrophotometer in the range of $4000\text{--}400\text{ cm}^{-1}$. The Brunauer–Emmett–Teller surface area (S_{BET}), total pore volume (V), and average pore radius (R) were determined by the ASAP2020 instrument using the Barrett–Joyner–Halenda (BJH) method. The thermogravimetric analysis (TGA) was performed on a Perkin Elmer TGA-7 in N_2 flow and at a heating rate of $10^\circ\text{C}/\text{min}$. The morphology was characterized by scanning electron microscopy (SEM, JSM-6700 F, Japan). The zeta potentials of adsorbents were measured with Malvern Zetasizer Nano ZS90, through adding 5 mg sample in 10 mL NaCl solution (10^{-3} mol/L) at different pH values (adjusted with diluted HNO_3 or NaOH solution).

Adsorption Experiments

All adsorption experiments were carried out in the dark condition at ambient temperature. The suspension containing 300 mg/L ARG solution ($\text{pK}_a = 7.5$) and 2 g/L of adsorbent was magnetically stirred for 45 min. Then the suspension was centrifuged at 4300 rpm for 5 min. The clarified supernatant was analyzed by the UV-Vis spectrophotometer (Agilent 8453). The absorbance value of ARG was read at 503 nm, corresponding to the characteristic absorption peak of azo group.

To study the influence of the surface potential of adsorbents on the adsorption capacities, the adsorbents were treated by NaOH or HNO_3 solution ($\text{pH} = 1.0\text{--}13.0$). Then the treated adsorbents were used to adsorb the same concentration of ARG

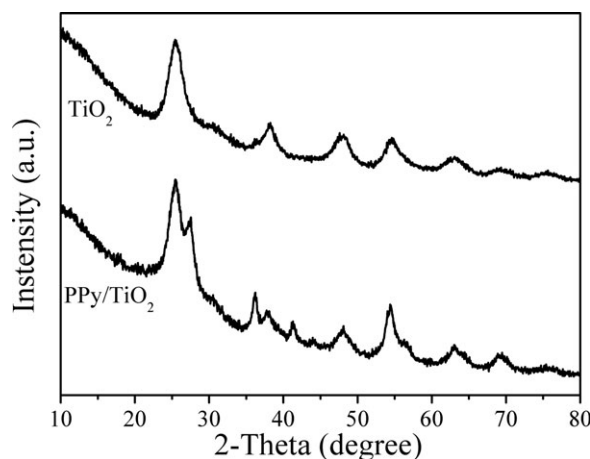


Figure 1. XRD patterns of the prepared TiO₂ and PPy/TiO₂.

solutions. The effect of ionic concentration (0–0.3 mol/L) on the adsorption was carried out by adding NaCl into the 300 mg/L ARG solution. The effect of PPy/TiO₂ dosage on the adsorption was examined by varying the adsorbent concentration from 0.5 to 3.0 g/L. The effect of temperature on the adsorption was also conducted by changing the temperature from 288 to 308 K.

The adsorption rate R (%) and the amount of dye molecules adsorbed onto adsorbent Q_t (mg/g) after time t were calculated from the following eqs. (1) and (2), respectively:

$$R(\%) = \frac{C_0 - C_t}{C_0} \times 100 \quad (1)$$

$$Q_t(\text{mg/g}) = \frac{C_0 - C_t}{M} \times V \quad (2)$$

where: C_0 is the initial dye concentration (mg/L), and C_t is the concentration of dye after time t ; V is the solution volume (L) and M is the mass of the used adsorbent (g).

The adsorption equilibrium of ARG with different concentrations (200, 300, and 500 mg/L) on PPy/TiO₂ was evaluated at 20°C, with 2 g/L of PPy/TiO₂ added and stirred for 1 h. The mixture was fetched per 10 min and filtered, and then the filtrates were analyzed by the UV-Vis spectrophotometer.

Equilibrium adsorption isotherms of ARG at 20°C were obtained by mixing different concentrations (150–450 mg/L) of ARG solution with 2 g/L of PPy/TiO₂. There are two models, Langmuir and Freundlich isotherms, which are described in the following eqs. (3) and (4), respectively:^{21,32}

$$\frac{C_{\text{eq}}}{Q_{\text{eq}}}(\text{g/L}) = \frac{1}{Q_{\text{max}}K_L} + \frac{C_{\text{eq}}}{Q_{\text{max}}} \quad (3)$$

$$\lg Q_{\text{eq}}(\text{mg/g}) = \lg K_F + n \lg C_{\text{eq}} \quad (4)$$

where: Q_{eq} and Q_{max} (mg/g) are the adsorbed dye equilibrium concentration in the solid phase and the maximum adsorption capacity, respectively; C_{eq} (mg/L) is the dye equilibrium concentration; K_L (L/mg) is a constant that related to the heat of adsorption; K_F ((mg/g)/(mg/L) ^{n}) represents the adsorption

capacity when C_{eq} equals 1; n represents the degree of dependence of adsorption on equilibrium concentration.

The ARG effluent (300 mg/L) was prepared by dissolving ARG into the real effluent instead of deionized water. The adsorption experiments of ARG effluent were the same as that of ARG solution, and the concentration of color was determined.

Regeneration Experiments

To test the regeneration abilities of the adsorbents, the used adsorbents were treated with 0.1 mol/L NaOH solution (5 mL) and 0.16 mol/L HNO₃ solution (5 mL) for 10 min sequentially. Then the regenerated adsorbent was reused for the further adsorption experiments.

RESULTS AND DISCUSSION

Characterization of the Samples

Figure 1 shows the XRD patterns of the prepared PPy/TiO₂ and TiO₂. The XRD pattern of TiO₂ shows the diffraction peaks at 25.3, 37.8, and 48.1°, which correspond well to the Bragg's reflections from the (101), (004), and (200) planes of anatase TiO₂, respectively. Additionally, the diffraction peaks at 27.5, 36.1, and 41.2° are found in the XRD pattern of PPy/TiO₂, with specific assignment to the (110), (101), and (111) planes of rutile TiO₂, respectively. These results indicated that the change of crystalline phase occurred during the process of the oxidative polymerization of PPy. It is also noted that no new peaks appear in the pattern of PPy/P25, suggesting that PPy is amorphous in the composite.³³

FTIR absorption spectra of TiO₂ and PPy/TiO₂ are shown in Figure 2. According to the spectrum of TiO₂, the wide peak at 400–700 cm^{−1} corresponds to Ti–O bending mode of TiO₂.³⁴ The spectrum of PPy/TiO₂ shows some characteristic peaks of PPy, for example, the bands at 1560, 1454, and 790 cm^{−1} are assigned to the pyrrole ring-stretching, the conjugated C–N stretching, and out-of-plane ring deformation of C–H, respectively.³⁵ However, the intensity of the peak at 400–700 cm^{−1} corresponded to Ti–O bending mode is lower, which may be because TiO₂ was largely enclosed by PPy. The spectrum of PPy/TiO₂ contains both the characteristic peaks of PPy and TiO₂, thus supporting the formation of PPy in the PPy/TiO₂ composites.

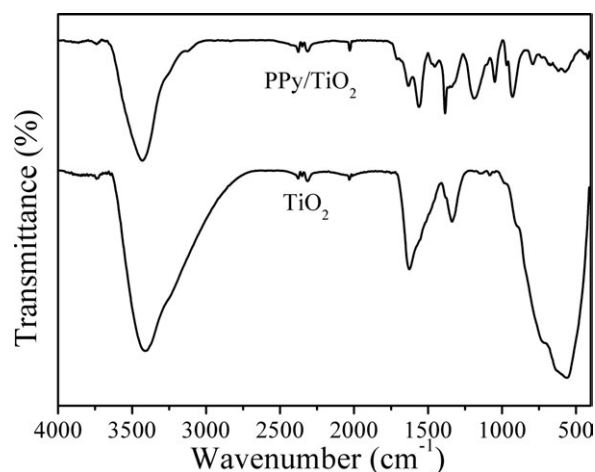


Figure 2. FTIR spectra of the prepared TiO₂ and PPy/TiO₂.

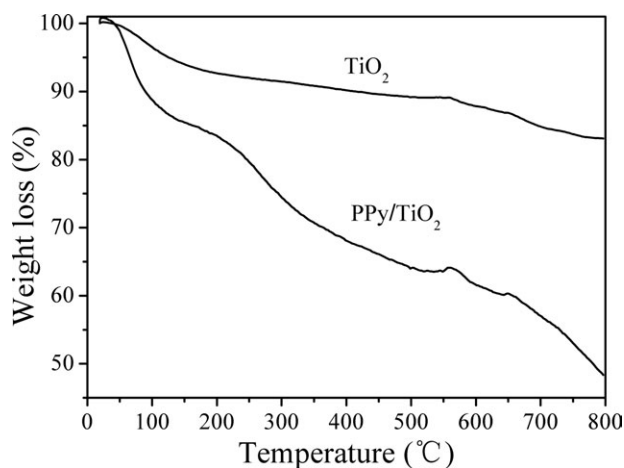


Figure 3. TGA curves of the prepared TiO_2 and PPy/TiO_2 .

As shown in TGA plots (Figure 3), the first steep weight loss of about 14% below 150°C for PPy/TiO_2 was attributed to the adsorbed water.³⁶ The second steep weight loss of about 22% between 200°C and 550°C may be assigned to the decomposition of PPy.³⁷ Based on the TGA analysis of PPy/TiO_2 , the amount of PPy in the PPy/TiO_2 composite was approximately calculated to be about 22 wt %.

Representative SEM images of TiO_2 and PPy/TiO_2 are illustrated in Figure 4. The pure TiO_2 was irregularly block structure. In comparison, the prepared PPy/TiO_2 composite existed as relatively loose aggregates with particle diameter of 5–7 μm . In addition, the loose aggregates were formed by the accumulation of large amounts of particles with the diameter of 100–200 nm. The modification of PPy led to the formation of the porous structure. Therefore, the specific surface areas of the samples were measured and the results are displayed in Table I. As observed, TiO_2 has a larger specific surface area ($S_{\text{BET}} = 87.92 \text{ m}^2/\text{g}$), which might be favorable for the efficient adsorption of ARG, but its average pore radius is comparatively small. It might be brought about by the sudden precipitation of large amounts of TiO_2 flocculent, which further affected the formation of pore structure due to the extrusion force between the molecules. By contrast, the average pore radius of PPy/TiO_2 is about three times larger than that of TiO_2 though its S_{BET} is smaller. This can be explained by the fact that the *in-situ* synthesized PPy deposited directly on the surface of TiO_2 , and thus decreased the specific surface area of TiO_2 , while the slow growth of PPy facilitated the formation of pore structure.

Effects of Surface Potential and Ionic Concentration on Adsorption

The adsorption capacities of the adsorbents were altered when they were treated with acid or alkali solution, as shown in Figure 5. The adsorption capacities of TiO_2 and PPy/TiO_2 increased with the decreasing pH, which proved that ARG could be easily adsorbed onto a lower pH treated adsorbent. Additionally, the alkaline and acid solutions would be used as the desorption agent and activating agent in the later regeneration experiments.

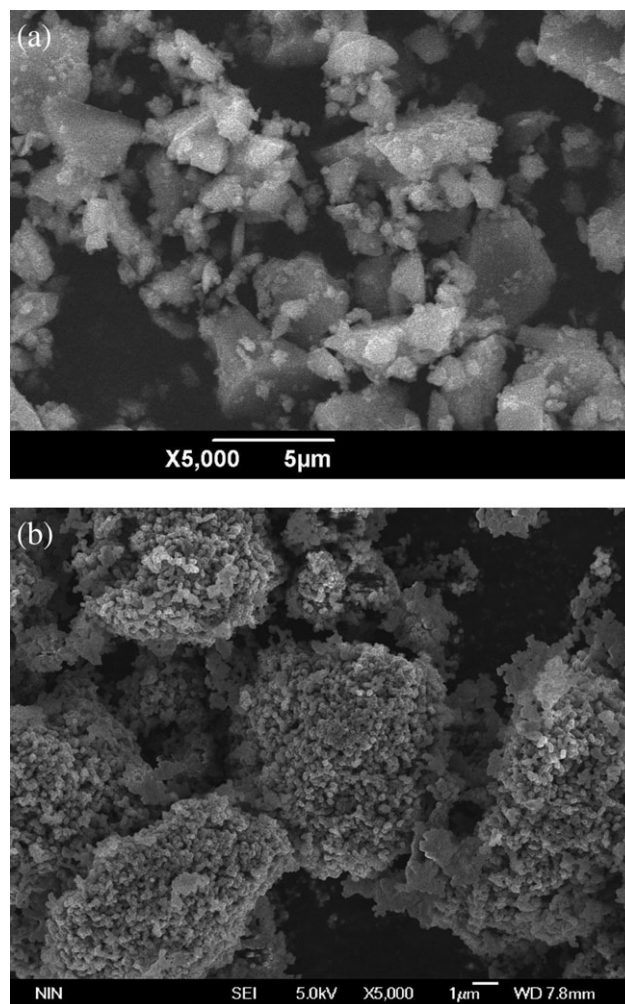
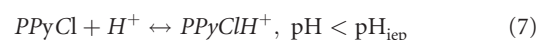
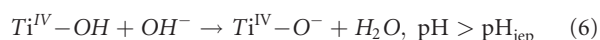
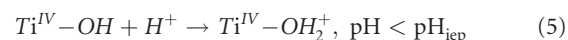


Figure 4. SEM images of the prepared (a) TiO_2 and (b) PPy/TiO_2 .

Several studies indicated that the surface charge of compound was greatly dependent on the pH of solution, and this affected its adsorption capacity.^{22,38} Belessi et al.⁵ and Zhang et al.³⁰ pointed out that the surfaces of TiO_2 and PPy were positively charged or negatively charged in a solution with an appropriate range of pH according to eqs. (5)–(8):



where pH_{iep} is the isoelectric point, which represents the pH value when the zeta potential equals to 0. Figure 6 shows the

Table I. Properties of Different Samples

Samples	S_{BET} (m^2/g)	V (cm^3/g)	R (nm)
TiO_2	87.92	0.053	1.56
PPy/TiO_2	53.51	0.14	5.67

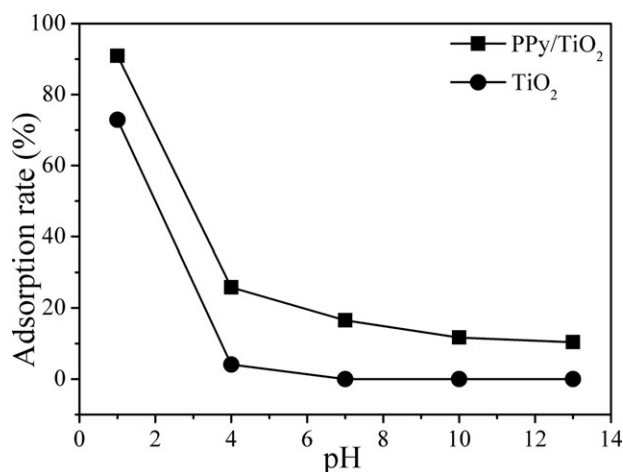


Figure 5. Effect of surface potential on adsorption capacities of the prepared TiO₂ and PPy/TiO₂. The adsorbents were treated with HNO₃ or NaOH solution (pH = 1.0–13.0).

zeta potential values of TiO₂ and PPy/TiO₂ as a function of the solution pH. The isoelectric points of TiO₂ and PPy/TiO₂ are about 2.8 and 10.5, respectively.

Therefore, the surface of PPy/TiO₂ was positively charged when the pH value of the solution was smaller than 10.0, and it could adsorb ARG through the electrostatic attraction. For TiO₂, it was negatively charged when the pH value of the solution was larger than 3.0, thus almost no ARG molecules could be adsorbed due to the existence of electrostatic repulsion. Furthermore, PPy/TiO₂ could still adsorb ARG when the pH value of the solution was 13, which may be owing to the formation of hydrogen bonding between PPy/TiO₂ and ARG. Consequently, PPy/TiO₂ exhibited better adsorption ability than TiO₂, and possessed adsorption ability within a larger pH range.

The effect of ionic concentration on the adsorption capacity is shown in Figure 7. The results showed that the effect of the ionic concentration was insignificant. Zhang et al.²⁶ indicated that the increase of ionic concentration reduced the electrostatic attraction between the adsorbates and adsorbents, and also reduced the electrostatic repulsion between the adsorbates. The first effect decreased the adsorption capacity, but the second

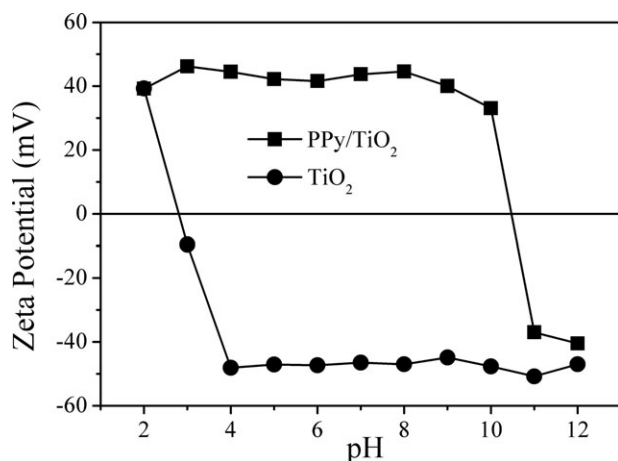


Figure 6. The zeta potentials of TiO₂ and PPy/TiO₂.

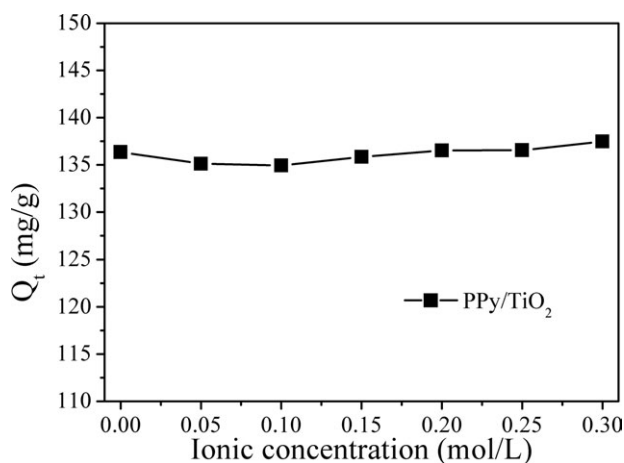


Figure 7. Effect of ionic concentration on the adsorption capacity of PPy/TiO₂.

effect enhanced the amount of adsorption. With the effects of these two aspects, the adsorption capacity of PPy/TiO₂ was almost unchanged at the different ionic concentration.

Effects of Dosage of Adsorbent and Temperature on Adsorption

The effect of PPy/TiO₂ dosage on the adsorption of ARG is shown in Figure 8(a). It was observed that the adsorption efficiency increased with the increase in dosage. The rise of the

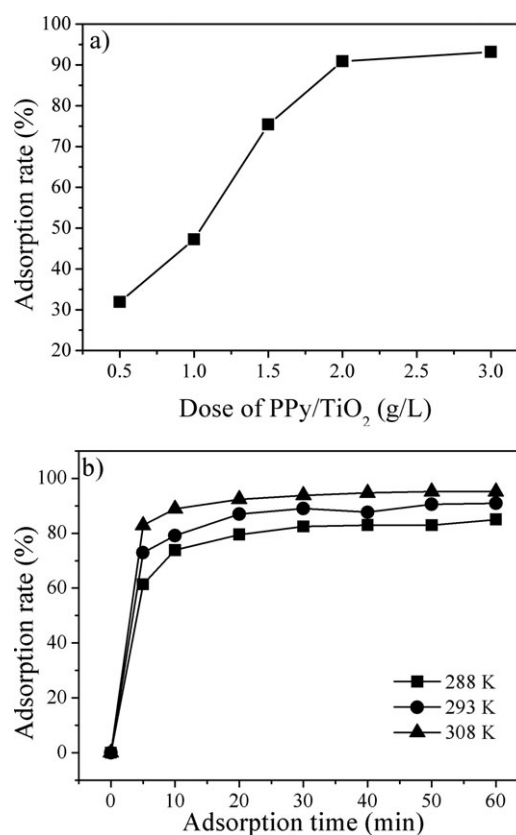


Figure 8. Effects of PPy/TiO₂ dosage and temperature on the adsorption of ARG.

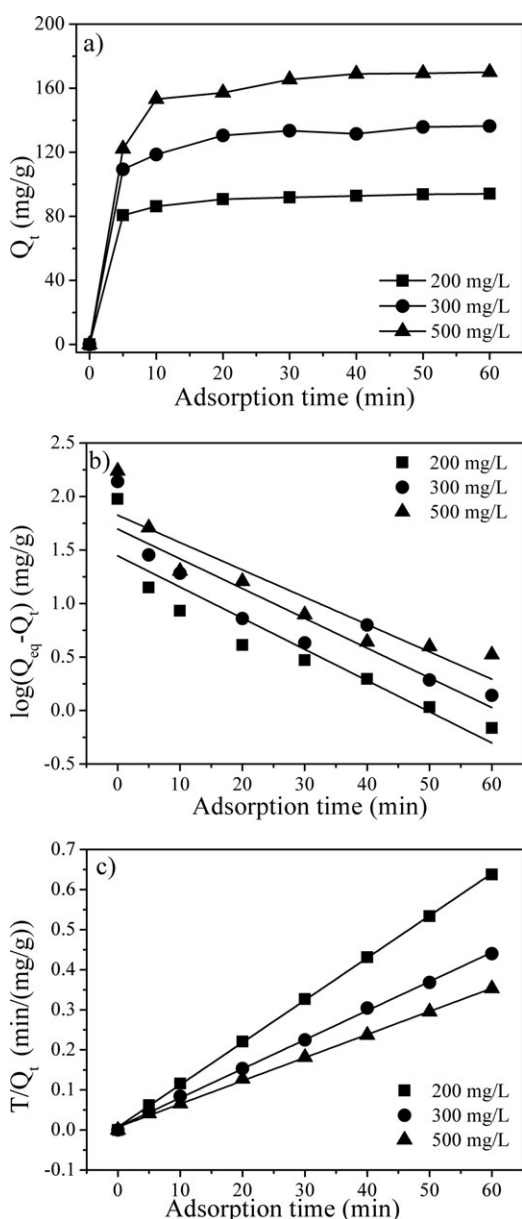


Figure 9. Adsorption capacity of PPY/TiO₂ for ARG. (a) Adsorption equilibrium curve of ARG; (b) Pseudo-first-order kinetic plot for the adsorption of ARG; (c) Pseudo-second-order kinetic plot for the adsorption of ARG.

adsorbent dosage can increase the number of active site available for adsorption, yet the adsorption efficiency had a little change when the dosage exceeded 2.0 g/L. As a result, the dosage of 2.0 g/L was chosen in all experiments.

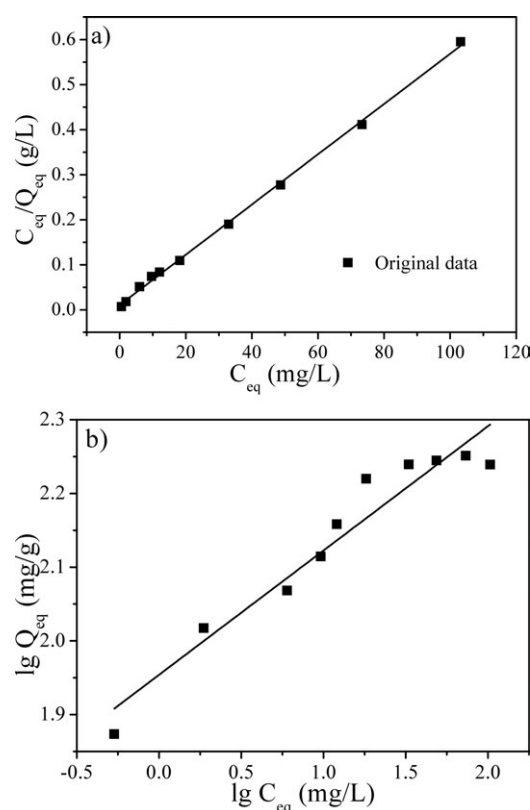


Figure 10. Adsorption isotherm of ARG on PPY/TiO₂, the liner forms for (a) Langmuir isotherm model and (b) Freundlich isotherm model.

The effect of temperature on the adsorption is displayed in Figure 8(b). It can be seen that the adsorption of ARG increased with the temperature rise, which indicated that adsorption of dye in this system was an endothermic process.

Adsorption Kinetics

It was essential that an adsorbent showed rapid adsorption kinetics for efficient adsorbate removal from solution. Figure 9(a) represents the influences of contact time and initial concentration on the adsorbed ARG on PPY/TiO₂. It is obvious that ARG adsorption was so rapid that a minimum contact time was sufficient for the removal of ARG from water. Therefore, it was feasible to choose 45 min as the adsorption time in the following adsorption experiments.

Moreover, the adsorption kinetics of ARG on PPY/TiO₂ was fitted by the pseudo-first-order model and pseudo-second-order model [as shown in Figure 9(b, c)], which are described in eqs. (9) and (10), respectively.³²

Table II. Parameters of the Pseudo-First-Order and Pseudo-Second-Order Models

C_0 (mg/L)	Pseudo first order model			Pseudo second order model		
	K_1 (1/min)	Q_{eq} (mg/g)	R^2	K_2 (g/mg/min)	Q_{eq} (mg/g)	R^2
200	0.067	27.94	0.8410	0.015	94.79	0.9997
300	0.064	49.70	0.8383	0.007	137.74	0.9991
500	0.059	66.99	0.8343	0.004	173.31	0.9990

Table III. Parameters of Langmuir and Freundlich Adsorption Isotherm Models

Langmuir model				Freundlich model		
Q_{\max} (mg/g)	K_L (L/mg)	R_L	R^2	K_F ((mg/g)(L/mg) $^{-n}$)	n	R^2
179.21	0.52	0.0043	0.9984	89.96	0.17	0.9257

$$\lg(Q_{\text{eq}} - Q_t) = \lg Q_{\text{eq}} - \frac{K_1}{2.303} T \quad (9)$$

$$\frac{T}{Q_t} = \frac{1}{K_2 Q_{\text{eq}}^2} + \frac{T}{Q_{\text{eq}}} \quad (10)$$

where T is the adsorption time (min), K_1 (1/min), and K_2 (g/mg/min) are the rate constants for the pseudo-first-order and pseudo-second-order models, respectively.

On the basis of Figure 9(b, c), the relevant parameters were calculated and listed in Table II. According to the values of the correlation coefficients, the pseudo-second-order model ($R^2 = 0.9990\text{--}0.9997$) was more appropriate for the adsorption kinetics of ARG with PPy/TiO₂ than the pseudo-first-order model ($R^2 = 0.8342\text{--}0.8410$). Furthermore, the calculated values of Q_{eq} from the pseudo-second-order model were approximately equal to the experimentally obtained values. These results indicated that the adsorption kinetics of ARG by PPy/TiO₂ could be well described by the pseudo-second-order model.

Adsorption Isotherms

In order to describe the interaction between the adsorbate and adsorbent, the equilibrium adsorption isotherm was investigated.³⁹ According to Figure 1, since its excellent adsorption ability, PPy/TiO₂ was chosen as the target adsorbent.

Figure 10 shows the linear forms of Langmuir and Freundlich adsorption isotherm models. It was clearly exhibited that the degree of linearity of Langmuir adsorption isotherm model was better than that of Freundlich adsorption isotherm model. To be more specific, the experimental parameters of Freundlich and Langmuir isotherm models are listed in Table III. It was obvious that the adsorption behavior of the PPy/TiO₂ sample was appointed to the Langmuir adsorption isotherm, for the correlation coefficient R^2 of Langmuir model was greater than that of Freundlich model.

Table IV. Comparison of the Adsorption Capacity of PPy/TiO₂ with Other Adsorbents for Azo Dyes

Adsorbents	Acid Red dyes	Q_{\max} (mg/g)	Equilibrium time (min)	References
PPy/TiO ₂	Acid Red G	179.21	20	This work
Activated carbon	Acid Red 97	52.08	30	40
CuFe ₂ O ₄ powder	Acid Red B	86.8	30	41
Montmorillonite	Acid Red G	171.53	60	42
Calcined-Alunite	Acid Red 57	80.02	120	43

According to the Langmuir model, the largest adsorption amount of ARG on PPy/TiO₂ adsorbent was 179.21 mg/g, which perhaps was no less than that of several other adsorbents. Table IV lists the adsorption capacities of several adsorbents for Acid Red dyes. It can be seen that the adsorption capacity of PPy/TiO₂ was satisfied when compared with some other adsorbents already reported in literatures. Besides, the equilibrium adsorption time of PPy/TiO₂ in our experiments was less than that of other adsorbents. These results suggested that the PPy/TiO₂ adsorbent we prepared had more efficient adsorption capacity, and can be considered as a promising adsorbent for the removal of dye from wastewater.

The dimensionless separation factor, R_L , which is an essential characteristic of the Langmuir model to define the favorability of an adsorption process, is expressed as

$$R_L = \frac{1}{1 + K_L C_m} \quad (11)$$

where C_m is the maximum initial concentration of ARG solution. The R_L value was calculated for the adsorption of ARG as 0.0043, which was in the range of 0–1, indicating the process of ARG adsorption on PPy/TiO₂ is favorable.

Regeneration Experiments

On the basis of the effect of the surface potential on the adsorption, the regeneration of TiO₂ and PPy/TiO₂ can be achieved by using NaOH solution (0.1 mol/L) as the desorption agent and HNO₃ solution (0.1 mol/L) as the activation agent. Afterwards, the regenerated adsorbents were utilized again to adsorb the same concentration of ARG solution to study its adsorption stability.

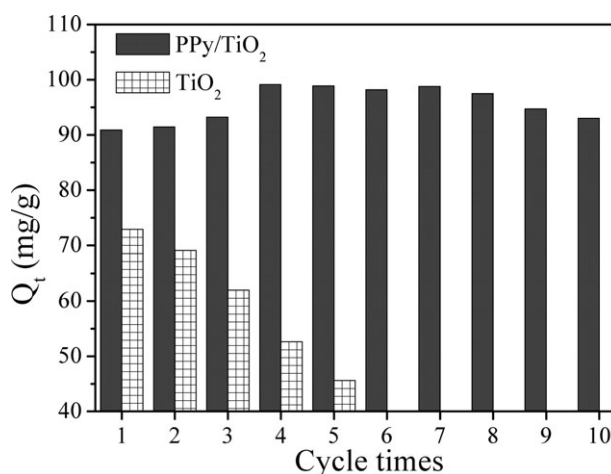


Figure 11. The adsorption stabilities of PPy/TiO₂ and TiO₂.

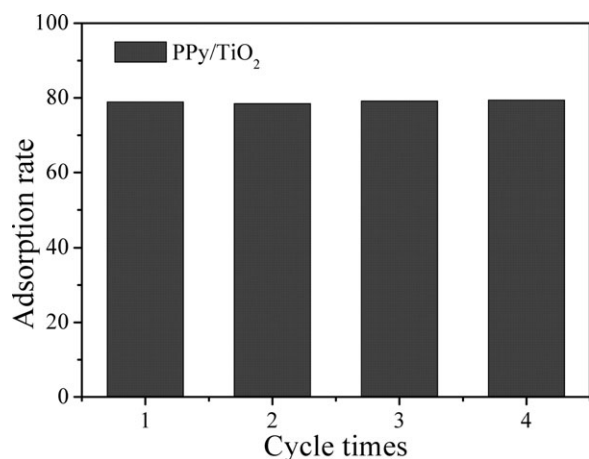


Figure 12. The adsorption efficiency of ARG effluent on PPy/TiO₂.

Figure 11 shows the adsorption stability of PPy/TiO₂ and TiO₂. It can be seen that the adsorption efficiency of PPy/TiO₂ was still higher than 90% after regeneration for ten times, indicating that this composite possessed excellent adsorption capacity and stability. In contrast, the adsorption capacity of TiO₂ showed a continuously decreasing trend. This suggested that the PPy modification can significantly improve the adsorption capacity and stability of TiO₂. Additionally, the amount of ARG adsorbed on the regenerated PPy/TiO₂ exceeded that on the virgin state with a trend of increase at first before declining afterwards. The rising trend was probably attributed to the activation of PPy/TiO₂ during the generation process, in which the quantity of positive charge of the regenerated adsorbent lifted, followed by a reinforced electrostatic attraction and improved adsorption of ARG. The slight decrease of the adsorption capacity may be owing to the incomplete desorption of ARG adsorbed on PPy/TiO₂. It was reported that the regeneration efficiency of activated carbon was only 50% to its original value or even less.^{9,16} These results demonstrated that the PPy/TiO₂ adsorbent we prepared could be completely regenerated via the alkali treatment and the acid treatment without losing its adsorption ability and stability.

Adsorption of Real Dye Wastewater

Figure 12 shows the decoloration efficiency of ARG effluent on PPy/TiO₂. The results showed that PPy/TiO₂ had weaker adsorption capacity for ARG effluent than for ARG solution, which may be ascribed to the complexity of the real effluent. However, the decoloration efficiency of ARG effluent on PPy/TiO₂ was still higher than 78% after adsorption–desorption for four times. These results indicated that PPy/TiO₂ also possessed efficient adsorption capacity for ARG in the real effluent.

CONCLUSIONS

In this article, the adsorption capacity of the prepared PPy/TiO₂ composite was studied and compared with TiO₂. PPy/TiO₂ was successfully prepared by *in-situ* chemical oxidative polymerization of pyrrole monomer in the prepared TiO₂ sol solution. XRD and FT-IR analyses suggested that PPy was incorporated

in the PPy/TiO₂ composite. The result from TGA analysis indicated that the amount of PPy in the PPy/TiO₂ composite was approximately calculated to be about 22 wt %. SEM analysis showed that the PPy/TiO₂ nanocomposite was rough and porous. Through the comparison of the adsorption properties of all samples for ARG, the acid-treated ones exhibit better adsorption effect, especially the acid-treated PPy/TiO₂ composite, which possessed an excellent adsorption capacity with the adsorption efficiency of more than 90% for 300 mg/L of ARG solution. Moreover, the effect of the ionic concentration on the adsorption was insignificant. Higher PPy/TiO₂ dosage and temperature were in favor of the adsorption of ARG. The equilibrium adsorption of ARG on PPy/TiO₂ was achieved in a short time of 20 min. Its adsorption kinetics was well described by the pseudo-second-order model. The Langmuir isotherm model was found for PPy/TiO₂ with the maximum adsorption amount of 179.21 mg/g. In addition, the adsorption stability experiments showed that PPy/TiO₂ could be *in-situ* regenerated by using NaOH as the desorption agent and HNO₃ as the activating agent, but the adsorption stability of TiO₂ was not perfect, which suggested that the modification of PPy was available. PPy/TiO₂ still showed excellent adsorption capacity after regeneration for ten times. Additionally, PPy/TiO₂ still possessed outstanding adsorption capacity for ARG effluent after regeneration for four times. Therefore, we believe that the PPy/TiO₂ composite is promising in the removal of azo dye from the wastewater.

ACKNOWLEDGMENTS

The authors gratefully acknowledge the financial supports from the Fundamental Research Funds for the Central Universities of China and the Specialized Research Fund for the Doctoral Program of Higher Education of China (20090201110005) and Natural Science Foundation of Jiangsu Province of China (SBK201022919, SBE201038213). They are also thankful for the preliminary editing effort and comments made by Prof. Charles Chou. Jingjing Li did the main part of the experiments and analyzed the results, and also wrote this manuscript. Jiangtao Feng took part in the synthesis and analysis work and guided the writing of the manuscript. Wei Yan provided the fund and guided the whole research. Wei Yan is also the corresponding author. All authors read and approved the final manuscript.

REFERENCES

- Crini, G. *Dyes Pigment.* **2008**, *77*, 415.
- Hameed, B. H.; Ahmad, A. L.; Din, A. T. M. *J. Hazard. Mater.* **2007**, *141*, 819.
- Al-Degs, Y. S.; El-Barghouthi, M. I.; El-Sheikh, A. H.; Walker, G. M. *Dyes Pigment.* **2008**, *77*, 16.
- Forgacs, E.; Cserh ti, T.; Oros, G. *Environ. Int.* **2004**, *30*, 953.
- Belessi, V.; Romanosa, G.; Boukosa, N.; Lambropouloud, D.; Trapalis, C. *J. Hazard. Mater.* **2009**, *170*, 836.
- Wang, S. B.; Zhu, Z. H. *Dyes Pigment.* **2007**, *75*, 306.
- Hameed, B. H.; Ahmad, A. L.; Latiff, K. N. A. *Dyes Pigment.* **2007**, *75*, 143.

8. Feng, T.; Zhang, F.; Wang, J.; Wang, L. *J. Appl. Polym. Sci.* **2012**, *125*, 1766.
9. Lazaridis, N. K.; Karapantsios, T. D.; Georgantas, D. *Water Res.* **2003**, *37*, 3023.
10. Yang, N.; Zhu, S. M.; Zhang, D.; Xu, S. *Mater. Lett.* **2008**, *62*, 645.
11. Elizalde-González, M. P.; Mattusch, J.; Wennrich, R. *Biore-sour. Technol.* **2008**, *99*, 5134.
12. Mall, I. D.; Srivastava, V. C.; Agarwal, N. K. *Dyes Pigm.* **2006**, *69*, 210.
13. Weng, C. H.; Hsu, M. C. *Sep. Purif. Technol.* **2008**, *64*, 227.
14. Lu, P. J.; Lin, H. C.; Yu, W. T.; Chern, J. M. *J. Taiwan Inst. Chem. Eng.* **2011**, *42*, 305.
15. Tanthapanichakoon, W.; Ariyadejwanich, P.; Japthong, P.; Nakagawa, K.; Mukai, S. R.; Tamon, H. *Water Res.* **2005**, *39*, 1347.
16. Janus, M.; Choina, J.; Morawski, A. W. *J. Hazard. Mater.* **2009**, *166*, 1.
17. Tan, X. L.; Fang, M.; Li, J. X.; Lu, Y.; Wang, X. K. *J. Hazard. Mater.* **2009**, *168*, 458.
18. Pérez León, C.; Kador, L.; Peng, B.; Thelakkat, M. *J. Phys. Chem. B* **2006**, *110*, 8723.
19. Asuha, S.; Zhou, X. G.; Zhao, S. *J. Hazard. Mater.* **2010**, *181*, 204.
20. Bourikas, K.; Styliidi, M.; Kondarides, D. I.; Verykios, X. E. *Langmuir* **2005**, *21*, 9222.
21. Janus, M.; Kusiak, E.; Choina, J.; Ziebro, J.; Morawski, A. W. *Desalination* **2009**, *249*, 359.
22. Wang, W. Y.; Ku, Y. *Colloids Surf., A* **2007**, *302*, 261.
23. Ishihara, T.; Misumi, Y.; Matsumoto, H. *Micropor. Mesopor. Mater.* **2009**, *122*, 87.
24. Cheng, Q. L.; He, Y.; Pavlinek, V.; Li, C. Z.; Saha, P. *Synth. Met.* **2008**, *158*, 953.
25. Karthikeyan, M.; Satheeshkumar, K. K.; Elango, K. P. *J. Hazard. Mater.* **2009**, *167*, 300.
26. Zhang, X.; Bai, R. B. *J. Mater. Chem.* **2002**, *12*, 2733.
27. Zhang, X.; Bai, R. B.; Tong, Y. W. *Sep. Purif. Technol.* **2006**, *52*, 161.
28. Bajpai, S. K.; Rohit, V. K.; Namdeo, M. *J. Appl. Polym. Sci.* **2009**, *111*, 3081.
29. Ansari, R.; Keivani, M. B.; Delavar, A. F. *J. Appl. Polym. Sci.* **2011**, *122*, 804.
30. Zhang, X.; Bai, R. B. *Langmuir* **2003**, *19*, 10703.
31. Pei, Q. B.; Qian, R. Y. *Synth. Met.* **1991**, *45*, 35.
32. Órfão, J. J. M.; Sliva, A. I. M.; Pereira, J. C. V.; Barata, S. A.; Fonseca, I. M.; Faria, P. C. C.; Pereira, M. F. R. *J. Colloid Interface Sci.* **2006**, *296*, 480.
33. Wang, D. S.; Wang, Y. H.; Li, X. Y.; Luo, Q. Z.; An, J.; Yue, J. X. *Catal. Commun.* **2008**, *9*, 1162.
34. Li, X. Y.; Wang, D. S.; Cheng, G. X.; Luo, Q. Z.; An, J.; Wang, Y. H. *Appl. Catal. B* **2008**, *81*, 267.
35. Feng, X. M.; Sun, Z. Z.; Hou, W. H.; Zhu, J. *J. Nanotechnol-ogy* **2007**, *18*, 195603.
36. Lai, C.; Li, G. R.; Dou, Y. Y.; Gao, X. P. *Electrochim. Acta* **2010**, *55*, 4567.
37. Omastová, M.; Trchová, M.; Kovářová, J.; Stejskal, J. *Synth. Met.* **2003**, *138*, 447.
38. Guzman, K. A. D.; Finnegan, M. P.; Banfield, J. F. *Environ. Sci. Technol.* **2006**, *40*, 7688.
39. Bhaumik, M.; Maity, A.; Srinivasu, V. V.; Onyango, M. S. *J. Hazard. Mater.* **2011**, *190*, 381.
40. Gómez, V.; Larrechi, M. S.; Callao, M. P. *Chemosphere* **2007**, *69*, 1151.
41. Wu, R. C.; Qu, J. H.; He, H.; Yu, Y. B. *Appl. Catal. B: Envi-ron.* **2004**, *48*, 49.
42. Tong, D. S.; Zhou, C. H.; Lan, Y.; Yu, H. Y.; Zhang, G. F.; Yu, W. H. *Appl. Clay Sci.* **2010**, *50*, 427.
43. Tunali, S.; Özcan, A. S.; Özcan, A. Gedikbey, T. *J. Hazard. Mater.* **2006**, *135*, 141.